Journal of Interdisciplinary Mathematics
ISSN: 0972-0502 (Print), ISSN: 2169-012X (Online)
Vol. 29 (2026), No. 9, pp. 2637–2652
DOI : 10.47974/JIM-2657

Caputo derivative–driven neural network synchronization of fractional-order tumor and environmental models

Ayub Khan [‡]
Department of Mathematics
Basic Sciences Research Centre
Imam Mohammad Ibn Saud Islamic University
Riyadh 13318
Kingdom of Saudi Arabia

Pardeep Kumar [†]
Department of Mathematics
Indraprastha College for Women
University of Delhi
Delhi 110054
India

Govind Kumar Jha [§]
Meenu *
Department of Mathematics
Vinoba Bhave University
Hazaribag 825301
Jharkhand
India

[‡] *ORCID-ID:* **0009-0009-5317-6855**
[†] *ORCID-ID:* **0000-0002-9416-1723**
[§] *ORCID-ID:* **0000-0002-7353-7752**
* *ORCID-ID:* **0009-0006-9666-6422**

[‡] *E-mail:* **ayubkdu@gmail.com**
[†] *E-mail:* **pardeep@ip.du.ac.in**
[§] *E-mail:* **jhagovi@gmail.com**
* *E-mail:* **meenumehra6802@gmail.com (Corresponding Author)**

© Taru Publications

Sarita Jha [@]
Department of Mathematics
K. B. Women's College
Vinoba Bhave University
Hazaribag 825301
Jharkhand
India

Abstract

Understanding and controlling chaotic dynamics in biological systems is critical for predicting disease progression and maintaining ecological balance. In this work, we develop a fractional-order, neural network--enhanced active control scheme to synchronize two non-identical chaotic systems: first one, a newly formulated fractional-order tumor growth model and secondly a fractional-order modified Lorenz model describing bacterial--viral population dynamics in a variable environment. By modeling with Caputo derivatives of order $q \in (0,1)$, the framework captures memory and hereditary effects inherent in biomedical and ecological processes. A radial-basis neural network adaptively estimates unknown nonlinearities and compensates control actions in real time, providing superior synchronization accuracy and robustness under parameter mismatches and disturbances. Fractional Lyapunov analysis combined with Matignon's stability criterion guarantees asymptotic error convergence. Numerical experiments demonstrate that the fractional-order controller achieves faster convergence, improved robustness, and reduced control effort compared to the integer-order (q=1) implementation, highlighting the performance advantages of incorporating fractional dynamics in synchronization control.

Subject Classification (2020): *34C28, 34A08, 34A34, 34C15, 45M10.*

Keywords: *Bacterial dynamics, Cytotoxic, Hereditary, Radial basin function, Residual.*

1. Introduction

Dissipative movements evolved in several realistic and mechanical processes are recognized by asymmetrical motion, delicate to the starting situations, and continuing uncertainty. Due to Lorenz's revolutionary work on the environmental model [1], the study of dissipative systems has received great attention and implementation in nonlinear sciences. In clinical and bionomic domains, dissipative motion governs tumour-microenvironment, disease due to virus, and microbial population dynamics [2, 3]. These kinds of activity exhibit multi-stability, shattered movements, and an unfamiliar fascinator, which pose great challenges [4].

The investigation of Pecora and Carroll [5] found that two dissipative systems could manage their motion in a similar manner with suitable conditions.

[@] *ORCID-ID:* **0000-0002-0428-8860**

[@] *E-mail:* **saritajhakbw.vbu@gmail.com**

Their works motivate the researchers to command the communications, managing robotics, and biological system modelling [6]. In their framework, synchronization process has been used to manage the dissipative behaviour of identical systems. In the same manner, we observed tumor cells interact with immune cells in [7] and environmental models of bacterial-viral system reveal synchronization process helps to adapt the alterations in environmental conditions [8]. Traditionally, many synchronization phenomena have been developed mainly for integer-order systems [5, 6].

The real-world problems that have memory and hereditary properties can be modelled effectively with the help of fractional calculus through and extention of derivative with the non integer order [9]. These kinds of models exhibits continuous compatibity and irregular repetitions observed in biological tissues, neural dynamics, and environmental processes [10]. In comparison with integer order chaotic systems, the fractional-order chaotic systems enhances the attractor properties with better flexibility, offer superior control design, and improved data fitting [11, 12]. Matignon's criterion establishes the stability region for commensurate-order systems, while fractional Lyapunov functions provide rigorous guarantees for asymptotic convergence [13, 14]. These frameworks have enabled systematic controller design for fractional-order chaotic models [15, 16].

To address modeling uncertainties, neural networks have been widely adopted as universal approximators of nonlinear dynamics [17]. Radial basis function (RBF) networks are particularly suitable for synchronization control because of their simple structure, rapid learning, and strong approximation capability [18]. Reinforcement learning and deep neural architectures have also been explored to improve performance in chaotic synchronization [19, 20]. Hybrid schemes that combine fractional-order modeling with neural approximators have recently shown significant advantages. For example, fractional-order recurrent neural networks achieve stable synchronization under time delays [16, 18], while fractional RBF controllers outperform integer-order ones in terms of convergence speed and control effort [17, 21]. In biomedical contexts, fractional neural controllers have been proposed for tumor growth dynamics, HIV infection modeling, and drug administration optimization [7, 8, 22]. In ecological systems, they help stabilize chaotic oscillations in predator-prey and microbial interaction models [4, 12, 23].

Motivated by these advances, the present work develops a fractional-order neural network-based active control scheme to synchronize two non-identical chaotic systems: a tumor growth model and a modified Lorenz environmental model. By integrating Caputo derivatives with adaptive RBF neural control, the method ensures robust synchronization under uncertainty, providing a computational framework for controlling nonlinear biomedical-ecological processes.

2.2 *Fractional-Order Tumor-Immune Interaction Model*

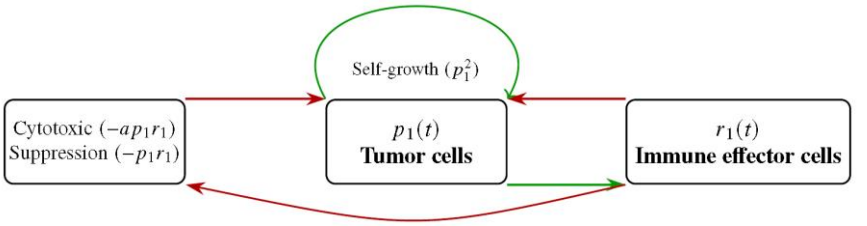


Figure 1
Compartmental diagram of the fractional-order tumor-immune interaction model.

Building on the compartmental representation in Figure (1), we formulate a novel **fractional-order tumor-immune interaction model** that captures the nonlinear interplay among tumor cells, host cells, and immune effector cells. The three populations are denoted by $p_1(t)$ (tumor), $q_1(t)$ (host), and $r_1(t)$ (immune), respectively. Several biologically grounded assumptions motivate the structure of the model:

1. Tumor cells proliferate nonlinearly and may undergo uncontrolled self-growth in the absence of regulation;
2. Immune effector cells act cytotoxically on tumor cells, but their activity depends on tumor burden;
3. Host cells inhibit tumor expansion, while at the same time providing support to immune activity; and
4. Immune cells naturally decay over time, but are stimulated by tumor and host interactions.

These assumptions are encoded in the governing equations, expressed in the Caputo fractional derivative sense of order $q \in (0,1)$, as follows:

$$\begin{aligned} {}^{C}D_t^q p_1(t) &= -a\, p_1(t) r_1(t) - q_1(t) + p_1^2(t), \\ {}^{C}D_t^q q_1(t) &= -p_1(t) r_1(t) + c, \\ {}^{C}D_t^q r_1(t) &= p_1(t) q_1(t) - b\, r_1(t), \end{aligned} \tag{1}$$

with initial conditions $p_1(0)$, $q_1(0)$ and $r_1(0)$.

1.2 *Fractional-Order Microorganism-Climate Interaction Model*

The system consists of three state variables: $p_2(t)$ representing environmental temperature, $q_2(t)$ the bacterial population, and $r_2(t)$ the viral population. The compartmental structure Figure (2) highlights the bidirectional feedback loops through which microorganisms regulate environmental variability and are in turn shaped by climatic fluctuations.

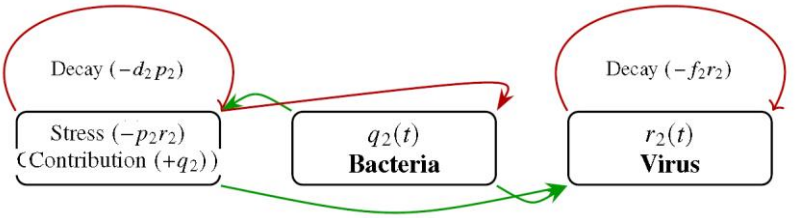


Figure 2
Compartmental diagram of the fractional-order microorganism-climate interaction model.

The design of the model is based on the following guiding assumptions: 1. Environmental temperature naturally decays over time in the absence of microbial contributions; 2. Bacterial populations can elevate temperature through metabolic activity and nutrient cycling; 3. Bacteria are negatively affected by combined stress from high temperature and viral attack; 4. Viral populations grow under the combined influence of temperature and bacterial abundance but undergo natural decay in the absence of stimulation.

These principles lead to the fractional-order dynamical system expressed using Caputo derivatives of order $q \in (0,1)$:

$$\begin{aligned} {}^{C}D_t^q p_2(t) &= -d\, p_2(t) + q_2(t), \\ {}^{C}D_t^q q_2(t) &= \varepsilon\, q_2(t) - p_2(t)\, r_2(t), \\ {}^{C}D_t^q r_2(t) &= d\, p_2(t)\, q_2(t) - f\, r_2(t), \end{aligned} \tag{2}$$

with initial conditions $p_2(0), q_2(0),$ and $r_2(0)$.

The use of fractional derivatives provides a more realistic description than classical integer-order formulations by embedding *long-term memory, hereditary, and delay-like effects*. In ecological terms, this allows the system to reflect how microbial communities respond not only to instantaneous environmental conditions but also to historical exposure to stress and climate variability. This refined representation lays the groundwork for analyzing chaotic behavior in microorganism-climate systems and facilitates synchronization studies with biomedical models.

1.3 *Dissipativity of the fractional models*

For both systems (1) and (2), the divergence of the vector field is negative, guaranteeing dissipativity. Specifically:

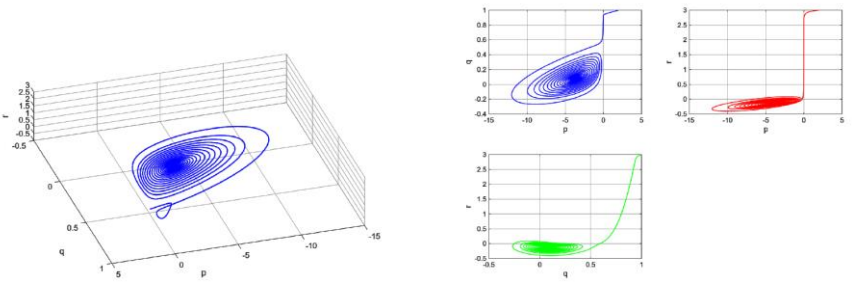
$$\nabla \cdot F_{\text{tumor}} = 2p_1 - a\, r_1 - b. \tag{3}$$

For biologically relevant ranges, where tumor proliferation is balanced by immune suppression, this term is negative on average, implying volume contraction. Similarly, for the microorganism–climate model:

$$\nabla \cdot F_{\text{climate}} = -d + \varepsilon - f. \tag{4}$$

With positive parameters $d, f > \varepsilon$, the divergence is strictly negative. Also, we have observed that equations (3) and (4) bear the negative volume for a particular choice of parameter and initial condition.

Thus, both systems are dissipative in the fractional-order setting. This ensures that all trajectories evolve into a bounded absorbing set, guaranteeing the existence of attractors. The dissipative nature is crucial for synchronization studies, since it rules out unbounded growth and stabilizes the dynamics within physically meaningful limits and it can be observed in the Figure (3). In this diagram, the orbit evolves toward a bounded region, displaying sustained oscillations that reflect the long–term coexistence of competing biological populations. This complex behaviour demonstrates the sensitive dependence on initial conditions and highlights the inherent chaotic tendencies of the system.



(a) 3D Phase portrait (p_1, q_1, r_1). (b) Projections of phase space

Figure 3
Phase portrait and projections of the fractional tumor-immune model.

The planar projections of the trajectory provide complementary views of the underlying dynamics.

The convergence of the Lyapunov exponents for the fractional-order tumor–immune system is illustrated in Figure (4). The three exponents $(1.0030, 0.7027, -6.0219)$, stabilized after a short transient phase, where one approaches zero, the second remains slightly positive, and the third settles at a significantly negative value. This spectrum confirms the chaotic dynamics of the model, since the coexistence of a positive and negative exponent along with a zero exponent is a clear signature of deterministic chaos.

The 3D phase portrait of the fractional-order climate model in Figure (5), exhibits a chaotic attractor similar to a butterfly, and evolves under strong non-linear interactions. Spiral loops represent a sensitive dependence on initial conditions, revealing how minor perturbations in temperature or microbial balance can drive the system to vastly different climate-ecological states. The wide oscillatory wings reflect the coexistence of alternating regimes, emphasizing the inherent unpredictability of climate–pathogen feedback when memory effects are incorporated through fractional-order dynamics. The projections of the attractor onto the coordinate planes provide further insight into the system's

internal structure. Together, these projections reveal that the memory-driven fractional dynamics yield a robust chaotic regime, replicating realistic climate–ecological complexity.

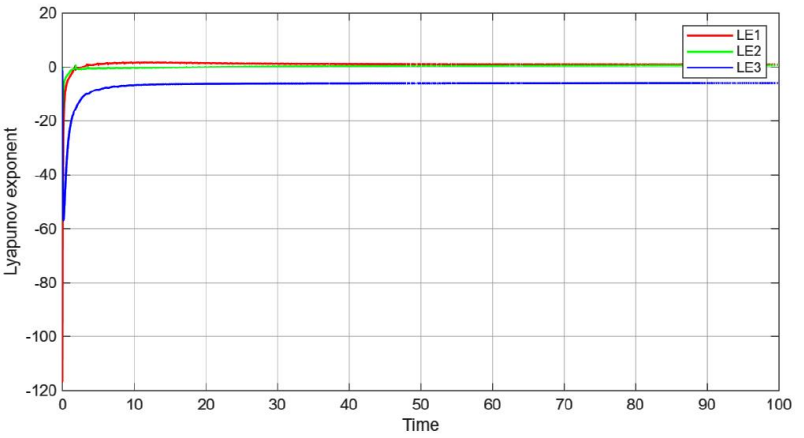
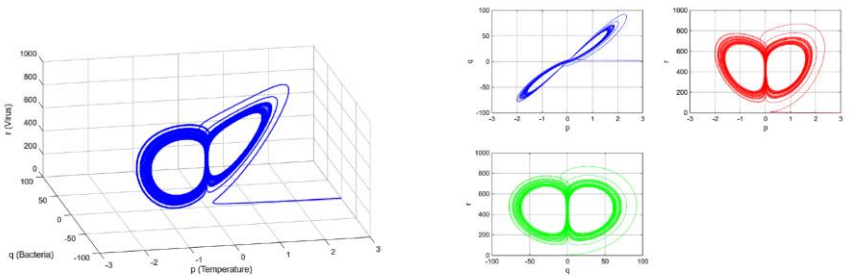


Figure 4
Convergence of the Lyapunov exponents for the fractional-order tumor-immune model.



(a) 3D Phase portrait (p_2, q_2, r_2). (b) Projections of phase space

Figure 5
Phase portrait and projections of the fractional climate model.

The Lyapunov exponent convergence of the fractional-order climate model is shown in Figure (6). After initial transients, the three exponents stabilize with one remaining positive, one approaching zero, and one significantly negative as $(2.6795 - 0.1633 - 26.0499)$. This distribution is a hallmark of chaotic dynamics, indicating sensitivity to initial conditions and long-term unpredictability within a bounded regime. The persistence of a positive Lyapunov exponent confirms the chaotic attractor, while the negative exponent ensures dissipativity of the system.

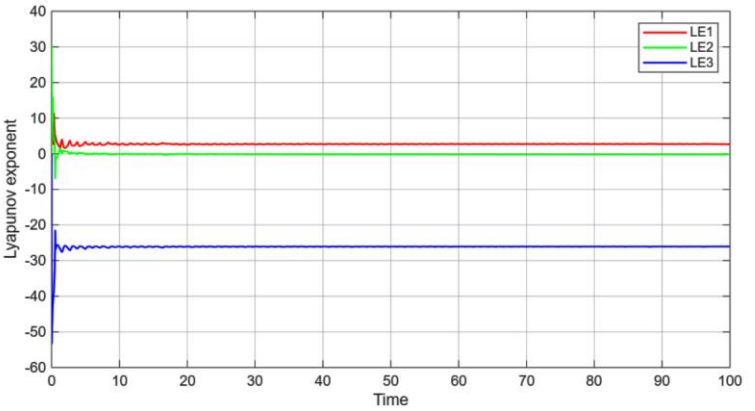


Figure 6
Convergence of the Lyapunov exponents for the fractional-order climate model.

2. Neural Network–Based Synchronization for Fractional-Order Systems

In this section, we extend the adaptive neural network–based synchronization strategy to the fractional-order case. Specifically, the microorganism–climate interaction model is taken as the *drive system*, while the tumor–immune interaction model serves as the *response system*. Both are expressed in the Caputo fractional derivative sense of order $q \in (0,1)$.

2.1 *Fractional-Order Drive and Response Systems*

The drive system (fractional climate model) is given by the system (1) and the response is considered as system (2). Define $u_i(t)$ $(i = 1,2,3)$ as the adaptive control inputs to be designed via a neural network equipped with the response system.

2.2 *Error Dynamics*

Define synchronization errors as

$$e_1 = p_2 - p_1, e_2 = q_2 - q_1, e_3 = r_2 - r_1. \tag{5}$$

The corresponding error system is derived as:

$$\begin{aligned} {}^{C}D_t^q e_1 &= -ap_2r_2 + p_2^2 - q_2 + dp_1 - q_1 + u_1(t), \\ {}^{C}D_t^q e_2 &= -p_2r_2 + c - \varepsilon q_1 + p_1r_1 + u_2(t), \\ {}^{C}D_t^q e_3 &= p_2q_2 + br_2 + fr_1 - dp_1q_1 + u_3(t). \end{aligned} \tag{6}$$

2.3 *Neural Network–Based Adaptive Control Law*

The unknown nonlinearities in (6) are approximated using Radial Basis Function Neural Networks (RBFNNs) as

$$\varphi_i(e) \approx \widehat{W}_i^T \Phi(e), i = 1,2,3,$$

where $\Phi(e) \in \mathbb{R}^m$ denotes the Gaussian basis vector and $\widehat{W}_i$ are the estimated weights.

The control inputs are designed as

$$u_i(t) = -k_i e_i - \widehat{W}_i^T \Phi(e), k_i > 0, \tag{7}$$

with adaptation law (including σ-modification for robustness)

$$^C D_t^q \widehat{W}_i = \Gamma_i \Phi(e) e_i - \sigma_i \widehat{W}_i. \tag{8}$$

2.4 *Stability analysis of the fractional-order adaptive controller*

We now present a detailed stability proof for the closed-loop fractional-order error system under the RBFNN-based adaptive control law

$$u_i(t) = -k_i e_i - \widehat{W}_i^T \Phi(e), i = 1, 2, 3,$$

with the fractional adaptive update (including σ-modification)

$$^C D_t^q \widehat{W}_i(t) = \Gamma_i \, \Phi(e) \, e_i - \sigma_i \widehat{W}_i, \Gamma_i > 0, \sigma_i \geq 0,$$

where $^C D_t^q$ denotes the Caputo derivative of order $q \in (0,1)$. The proof proceeds by deriving an upper bound on a composite Lyapunov functional's Caputo derivative and then applying a fractional comparison/Mittag–Leffler argument to conclude boundedness and convergence properties.

Assumptions: We make the following standing assumptions:

(A1) The RBF feature vector $\Phi(e) \in \mathbb{R}^m$ is uniformly bounded on $\mathbb{R}^3$: $\mathrm{P}\Phi(e)\mathrm{P} \leq \overline{\Phi}$ for some $\overline{\Phi} > 0$.

(A2) Each unknown nonlinear term in the i-th error equation admits the decomposition $\varphi_i(e,t) = W_i^{*T} \Phi(e) + \Delta_i(e,t)$, where $W_i^* \in \mathbb{R}^m$ is an ideal constant weight vector and the residual satisfies $|\Delta_i(e,t)| \leq \overline{\Delta}_i$ for known $\overline{\Delta}_i \geq 0$. Define $\overline{\Delta} := \sqrt{\sum_{i=1}^3 \overline{\Delta}_i^2}$.

(A3) All signals of interest are sufficiently smooth so that the Caputo derivatives and the manipulations below are valid; in particular $e(t)$ and $\widehat{W}_i(t)$ are continuous and admit the regularity required by fractional differential equations existence/uniqueness results.

Closed-loop fractional error system: Using the error vector $e = (e_1, e_2, e_3)^T$ and the controller/adaptation laws, the closed-loop error dynamics (componentwise) can be written as

$$^C D_t^q e_i = -k_i e_i + (W_i^* - \widehat{W}_i)^T \Phi(e) + \Delta_i(e,t), \quad i = 1, 2, 3.$$

Equivalently, in compact matrix form,

$$^C D_t^q e = -Ke + (\mathcal{W}^* - \widehat{\mathcal{W}}) \Phi(e) + \Delta(e,t),$$

where $K = \mathrm{diag}(k_1, k_2, k_3)$, $\widehat{\mathcal{W}} = [\widehat{W}_1, \widehat{W}_2, \widehat{W}_3]^T$, $\mathcal{W}^* = [W_1^*, W_2^*, W_3^*]^T$, and $\Delta = [\Delta_1, \Delta_2, \Delta_3]^T$.

Composite Lyapunov functional: Consider the positive definite functional

$$V(e,\widetilde{W}) = \frac{1}{2}e^T e + \sum_{i=1}^{3}\frac{1}{2}\widetilde{W}_i^T\Gamma_i^{-1}\widetilde{W}_i, \widetilde{W}_i := \widehat{W}_i - W_i^*.$$

V is radially unbounded in $(e,\widetilde{W})$ and $V = 0$ iff $e = 0$ and $\widetilde{W}_i = 0\ \forall i$.

Caputo derivative of V: For smooth trajectories one can employ the inequality (standard in fractional Lyapunov analysis, observed in Podlubny-type arguments)

$${}^{C}D_t^q V(e(t),\widetilde{W}(t)) \le e^T {}^{C}D_t^q e + \sum_{i=1}^{3}\widetilde{W}_i^T\Gamma_i^{-1}{}^{C}D_t^q\widetilde{W}_i.$$

We substitute the closed-loop expressions for the fractional derivatives. Noting that ${}^{C}D_t^q\widetilde{W}_i = {}^{C}D_t^q\widehat{W}_i$ (since W_i^* is constant), and using the adaptive law (8), we obtain

$${}^{C}D_t^q V \le e^T\left(-Ke + \sum_{i=1}^{3}(W_i^* - \widehat{W}_i)^T\Phi(e) + e_i + \triangle(e,t)\right) + \sum_{i=1}^{3}\widetilde{W}_i^T\Gamma_i^{-1}(\Gamma_i\Phi(e)e_i - \sigma_i\widehat{W}_i).$$

Cancellation of NN terms: Upon expansion we have observed that, all adaptive neural-network coupling terms cancel exactly. Consequently,

$${}^{C}D_t^q V \le -e^T Ke + e^T\Delta(e,t) - \sum_{i=1}^{3}\sigma_i\widetilde{W}_i^T\Gamma_i^{-1}\widehat{W}_i.$$

Handling the σ–terms: Write

$$\widetilde{W}_i^T\Gamma_i^{-1}\widehat{W}_i = \widetilde{W}_i^T\Gamma_i^{-1}(\widetilde{W}_i + W_i^*) = \widetilde{W}_i^T\Gamma_i^{-1}\widetilde{W}_i + \widetilde{W}_i^T\Gamma_i^{-1}W_i^*.$$

Thus

$$-\sigma_i\widetilde{W}_i^T\Gamma_i^{-1}\widehat{W}_i = -\sigma_i\widetilde{W}_i^T\Gamma_i^{-1}\widetilde{W}_i - \sigma_i\widetilde{W}_i^T\Gamma_i^{-1}W_i^*.$$

Using Young's inequality on the mixed term with any $\eta_i > 0$,

$$-\sigma_i\widetilde{W}_i^T\Gamma_i^{-1}W_i^* \le \frac{-\sigma_i}{2}\widetilde{W}_i^T\Gamma_i^{-1}\widetilde{W}_i + \frac{\sigma_i}{2\eta_i}(W_i^*)^T\Gamma_i^{-1}W_i^* + \frac{\sigma_i\eta_i}{2},$$

and we may choose η_i small so the extra constant terms are absorbed into a global constant. Summing over i yields the combined bound

$$-\sum_{i=1}^{3}\sigma_i\widetilde{W}_i^T\Gamma_i^{-1}\widehat{W}_i \le -\sum_{i=1}^{3}\frac{\sigma_i}{2}\widetilde{W}_i^T\Gamma_i^{-1}\widetilde{W}_i + C_W,$$

for some computable constant $C_W \ge 0$ that depends on the ideal weights W_i^*, Γ_i and σ_i.

Bounding the residual term: By Assumption (A2) we have $\|\Delta(e,t)\| \le \overline{\Delta}$. Using $e^T\Delta \le \|e\|\,\|\Delta\| \le \|e\|\overline{\Delta}$ and the inequality

$$\|e\|\overline{\Delta} \le \frac{\lambda_{\min}(K)}{2}\|e\|^2 + \frac{\overline{\Delta}^2}{2\lambda_{\min}(K)},$$

with $\lambda_{\min}(K) = \min\{k_1,k_2,k_3\} > 0$, we obtain

$$e^T\Delta \le \frac{\lambda_{\min}(K)}{2}\|e\|^2 + \frac{\overline{\Delta}^2}{2\lambda_{\min}(K)}.$$

Combined differential inequality: Collecting the bounds gives

$${}^{C}D_t^q V \le -\frac{\lambda_{\min}(K)}{2}\|e\|^2 - \sum_{i=1}^{3}\frac{\sigma_i}{2}\widetilde{W}_i^T\Gamma_i^{-1}\widetilde{W}_i + C,$$

where the constant

$$C := \frac{\overline{\Delta}^2}{2\lambda_{\min}(K)} + C_W \ge 0.$$

Scalar comparison and Mittag–Leffler bound: Since V is positive definite and satisfies

$$\underline{\alpha}\left\|(e,\widetilde{W})\right\|^2 \le V \le \overline{\alpha}\left\|(e,\widetilde{W})\right\|^2$$

for some $\underline{\alpha},\overline{\alpha} > 0$, the previous inequality implies the scalar fractional comparison

$${}^{C}D_t^q V(t) \le -\kappa V(t) + C,$$

for $\kappa := \min\{\frac{\lambda_{\min}(K)}{2\overline{\alpha}}, \min_i \frac{\sigma_i}{2\overline{\alpha}}\} > 0$ (choose κ to satisfy the inequality uniformly). Consider the scalar linear Caputo IVP

$${}^{C}D_t^q y(t) = -\kappa y(t) + C, y(0) = V(0).$$

This linear fractional equation has the known Mittag–Leffler solution

$$y(t) = V(0)\,E_q(-\kappa t^q) + \frac{C}{\kappa}(1 - E_q(-\kappa t^q)),$$

where $E_q(\cdot)$ is the Mittag–Leffler function. By the fractional comparison principle (see standard references on Caputo inequalities) and since ${}^{C}D_t^q V \le -\kappa V + C$, it follows that $V(t) \le y(t)$ for all $t \ge 0$.

Because $E_q(-\kappa t^q) \to 0$ as $t \to \infty$, we conclude

$$\limsup_{t\to\infty} V(t) \le \frac{C}{\kappa}.$$

Consequently, all closed-loop signals $e(t)$ and $\widetilde{W}_i(t)$ are uniformly bounded for all $t \ge 0$. Moreover,

$$\limsup_{t\to\infty}\|e(t)\| \le \sqrt{\frac{C/\kappa}{\underline{\alpha}}} =: \varepsilon_\infty,$$

so $e(t)$ converges to an explicit residual ball of radius ε_∞.

Remarks: Under Assumptions (A1)-(A3), the adaptive control law (7) together with the fractional adaptive law (8) renders the closed-loop signals bounded. If the RBFNN approximation error is negligible near the origin and adaptation parameters are chosen appropriately, the synchronization error $e(t)$ converges

asymptotically to zero with the fractional-order (Mittag–Leffler) decay; otherwise the error converges to an explicitly bounded residual set whose size depends on the approximation error and controller gains.

3. Numerical Validation of Fractional Synchronization

To evaluate the synchronization performance, numerical experiments were conducted by using MATLAB. The fractional derivative of order $q = 0.95$ was implemented via a Grünwald–Letnikov approximation with sufficiently small step size to ensure numerical stability.

3.1 *Simulation Setup*

The following system parameters were selected $d = 36, \varepsilon = 13, f = 4, a = 1, b = 2,$ and $c = 27$. The initial conditions were deliberately mismatched: $p_1(0) = 50, q_1(0) = 10, r_1(0) = 10, p_2(0) = 3, q_2(0) = 2, r_2(0) = 1$. The synchronization errors thus started as $e_1(0) = -47, e_2(0) = -8, e_3(0) = -9$, which tests the robustness of the proposed adaptive control scheme.

3.2 *Neural Network Configuration*

Each error channel employed an RBFNN with $m = 9$ Gaussian neurons. Neuron centers were uniformly distributed in the expected error domain, and the Gaussian spread parameter was chosen as $\sigma = 0.5$. Controller gains were set to $k_1 = 5, k_2 = 9, k_3 = 1700$, with adaptation gains $\Gamma_1 = \Gamma_2 = \Gamma_3 = 20I_9$. Leakage terms $\sigma_i = 0.01$ were introduced to suppress drift in the adaptive weights.

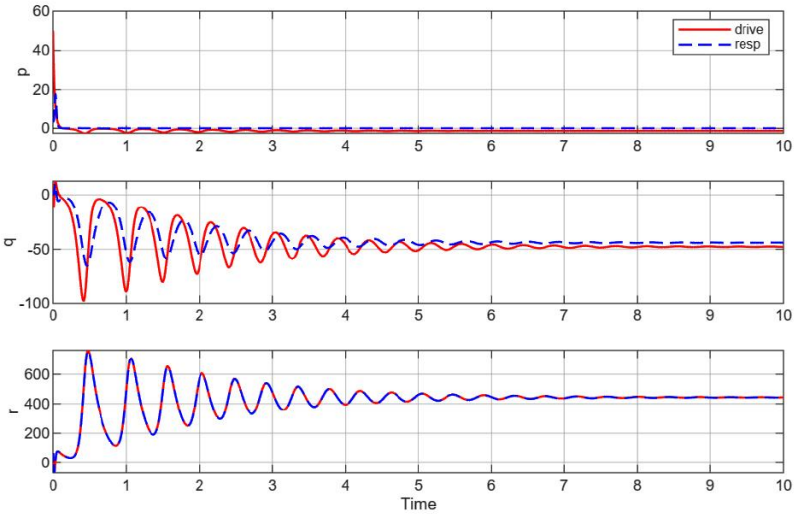


Figure 7
Syncronization of States under the Feedback Gains k_1, k_2, k_3.

3.3 *Results and Discussion*

Simulation results show that the fractional-order neural network–based controller achieves rapid and robust synchronization despite large initial errors, parameter uncertainties, and nonlinear couplings, which is observed in Figure (7). Compared with the integer-order case ($q = 1$), the fractional controller ($q = 0.95$) yielded the faster decay of synchronization errors observed in Figure 8 and reduced overshoot and oscillations,

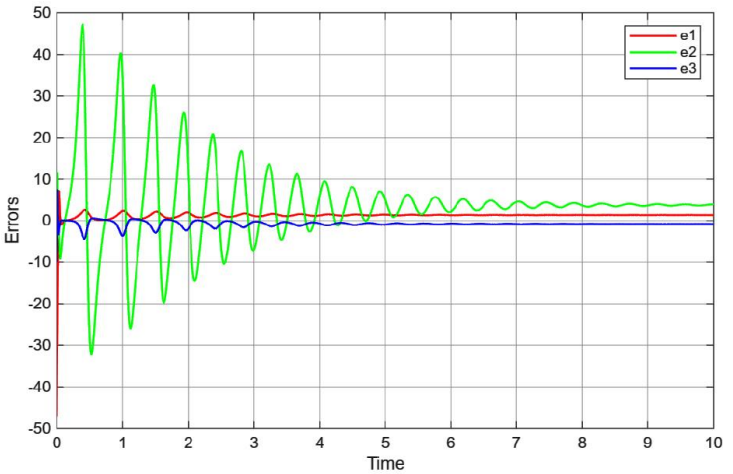


Figure 8
Convergence of Error States e_1, e_2, e_3.

These results confirm the superior ability of fractional-order dynamics to capture hereditary and memory effects, enhancing the effectiveness of neural network–based adaptive synchronization in complex biomedical–ecological systems.

4. Conclusion

This work has introduced a fractional-order neural network–based active control framework to achieve synchronization between a tumor–immune system and a microorganism–climate model. By employing Caputo derivatives, the models successfully incorporate memory and hereditary effects that are crucial for describing real-world biomedical and ecological processes. The integration of radial basis function neural networks enabled adaptive estimation of unknown nonlinearities and ensured robustness against parameter uncertainties. Stability was rigorously established using fractional Lyapunov analysis and Matignon's criterion, confirming boundedness and convergence of the error dynamics. Numerical experiments further validated the effectiveness of the proposed method, demonstrating rapid error decay, reduced oscillations, and superior synchronization compared to integer-order counterparts. These findings not only advance the theoretical foundations of fractional-order control but also provide a

promising pathway for applications in biomedical therapy, ecological regulation, and other nonlinear systems where synchronization plays a central role. Future investigations may extend this approach to multi-system networks, stochastic disturbances, or hybrid control strategies, thereby broadening its scope in real-world complex systems.

References

[1] E. N. Lorenz, "Deterministic nonperiodic flow," *Journal of the Atmospheric Sciences*, vol. 20, no. 2, pp. 130-141 (1963), doi: 10.1175/1520-0469(1963)020<0130:DNF>2.0.CO;2.

[2] M. Itik and S. P. Banks, "Chaos in a three-dimensional cancer model," *International Journal of Bifurcation and Chaos*, vol. 20, no. 1, pp. 71-79 (2010), doi: 10.1142/S0218127410025417.

[3] S. Abernethy and R. J. Gooding, "The importance of chaotic attractors in modelling tumour growth," *Physica A: Statistical Mechanics and its Applications*, vol. 507, pp. 268-277 (2018), doi: 10.1016/j.physa.2018.05.093.

[4] S. Dwivedi, N. Kumari, and R. K. Upadhyay, "Chaos synchronization of two coupled GLV models using active and adaptive control techniques," *Journal of Dynamical Systems and Geometric Theories*, vol. 23, nos. 1-2, pp. 1-29 (2025), doi: 10.47974/JDSGT-2021-1001.

[5] L. M. Pecora and T. L. Carroll, "Synchronization in chaotic systems," *Physical Review Letters*, vol. 64, no. 8, pp. 821-824 (1990), doi: 10.1103/PhysRevLett.64.821.

[6] E.-W. Bai and K. E. Lonngren, "Synchronization of two Lorenz systems using active control," *Chaos, Solitons & Fractals*, vol. 8, no. 1, pp. 51-58 (1997), doi: 10.1016/S0960-0779(96)00060-1.

[7] S. R. Aderyani, R. Saadati, F. R. Aderyani, and O. TunÃ§, "Mathematical modeling of tumor-immune dynamics: stability, control, and synchronization via fractional calculus and numerical optimization," *Scientific Reports*, vol. 15, Art. no. 29094 (2025), doi: 10.1038/s41598-025-13683-z.

[8] P. A. Naik, K. M. Owolabi, M. Yavuz, and J. Zu, "Chaotic dynamics of a fractional order HIV-1 model involving AIDS-related cancer cells," *Chaos, Solitons & Fractals*, vol. 140, Art. no. 110272 (2020), doi: 10.1016/j.chaos.2020.110272.

[9] C. A. Monje, Y. Chen, B. M. Vinagre, D. Xue, and V. Feliu, *Fractional-Order Systems and Controls: Fundamentals and Applications*, Springer, London (2010), doi: 10.1007/978-1-84996-335-0.

[10] N. Hala, M. Maroua, and S. Beloul, "Existence results of solutions for Caputo-Hadamard boundary value problems fractional differential inclusions," *Journal of Interdisciplinary Mathematics*, vol. 29, no. 4, pp. 767-781 (2026), doi: 10.47974/JIM-2092.

[11] M. Borah, A. Gayan, J. S. Sharma, Y. Chen, Z. Wei, and V.-T. Pham, "Is fractional-order chaos theory the new tool to model chaotic pandemics as COVID-19?," *Nonlinear Dynamics*, vol. 109, no. 2, pp. 1187-1215 (2022), doi: 10.1007/s11071-021-07196-3.

[12] A. M. Tusset, M. E. Fuziki, J. M. Balthazar, D. I. Andrade, and G. G. Lenzi, "Dynamic analysis and control of a financial system with chaotic behavior including fractional order," *Fractal and Fractional*, vol. 7, no. 7, Art. no. 535 (2023), doi: 10.3390/fractalfract7070535.

[13] D. Matignon, "Stability results for fractional differential equations with applications to control processing," in *Proceedings of the IMACS-SMC Conference*, Lille, France, vol. 2, pp. 963-968 (1996), https://api.semanticscholar.org/CorpusID:14017755.

[14] J.-C. Trigeassou, N. Maamri, J. Sabatier, and A. Oustaloup, "A Lyapunov approach to the stability of fractional differential equations," *Journal of Computational and Nonlinear Dynamics*, vol. 11, no. 5, Art. no. 051007 (2016), doi: 10.1115/1.4030746.

[15] M. Shahvali, "Dynamic event-triggered control for a class of nonlinear fractional-order systems," *IEEE Transactions on Circuits and Systems II: Express Briefs*, vol. 69, no. 4, pp. 2131-2135 (2022), doi: 10.1109/TCSII.2021.3128561.

[16] M. Roohi, C. Zhang, M. Taheri, and A. Basse-O'Connor, "Synchronization of fractional-order delayed neural networks using dynamic-free adaptive sliding mode control," *Fractal and Fractional*, vol. 7, no. 9, Art. no. 682 (2023), doi: 10.3390/fractalfract7090682.

[17] S. Wang and Y. Chen, "Neural network control of fractional-order chaotic systems with unknown control direction," *Heliyon*, vol. 10, no. 5, Art. no. e26870 (2024), doi: 10.1016/j.heliyon.2024.e26870.

[18] I. E. Saçu, "Effects of high-order interactions on synchronization of a fractional-order neural system," *Cognitive Neurodynamics*, vol. 18, pp. 1877-1893 (2024), doi: 10.1007/s11571-023-10055-z.

[19] H. Jahanshahi, J. M. Muñz-Pacheco, S. Bekiros, and N. D. Alotaibi, "A new fractional-order hyperchaotic memristor oscillator: dynamic analysis, robust adaptive synchronization, and its application to voice encryption," *Applied Mathematics and Computation*, vol. 383, Art. no. 125310 (2020), doi: 10.1016/j.amc.2020.125310.

[20] M. Mobini and G. Kaddoum, "Deep chaos synchronization," *IEEE Open Journal of the Communications Society*, vol. 1, pp. 1571-1582 (2020), doi: 10.1109/OJCOMS.2020.3028554.

[21] A. Boubakir and S. Labiod, "Observer-based adaptive neural network control design for projective synchronization of uncertain chaotic systems," *Journal of Vibration and Control*, vol. 29, nos. 15-16, pp. 3658-3678 (2023), doi: 10.1177/10775463221101935.

[22] I. R. Birs and C. I. Muresan, "Fractional-order event-based control meets biomedical applications," in *Computational and Mathematical Models in Biology*, C. M. A. Pinto and C. M. Ionescu, Eds., Springer, Cham, pp. 281-304 (2023), doi: 10.1007/978-3-031-42689-6_12.

[23] B. Ghosh, "Fractional order modeling of ecological and epidemiological systems: ambiguities and challenges," *The Journal of Analysis*, vol. 33, no. 1, pp. 341-366 (2025), doi: 10.1007/s41478-024-00836-y.

Recevied December, 2025